



**HAL**  
open science

## **Intrinsic quality analysis of binary partition trees**

Jimmy Francky Randrianasoa, Camille Kurtz, Pierre Gançarski, Eric Desjardin, Nicolas Passat

► **To cite this version:**

Jimmy Francky Randrianasoa, Camille Kurtz, Pierre Gançarski, Eric Desjardin, Nicolas Passat. Intrinsic quality analysis of binary partition trees. International Conference on Pattern Recognition and Artificial Intelligence (ICPRAI), 2018, Montréal, Canada. pp.114-119. hal-01695077

**HAL Id: hal-01695077**

**<https://hal.univ-reims.fr/hal-01695077v1>**

Submitted on 9 Feb 2018

**HAL** is a multi-disciplinary open access archive for the deposit and dissemination of scientific research documents, whether they are published or not. The documents may come from teaching and research institutions in France or abroad, or from public or private research centers.

L'archive ouverte pluridisciplinaire **HAL**, est destinée au dépôt et à la diffusion de documents scientifiques de niveau recherche, publiés ou non, émanant des établissements d'enseignement et de recherche français ou étrangers, des laboratoires publics ou privés.

# Intrinsic Quality Analysis of Binary Partition Trees

Jimmy Francky Randrianaso<sup>1</sup>, Camille Kurtz<sup>2</sup>, Pierre Gançarski<sup>1</sup>, Éric Desjardin<sup>3</sup>, Nicolas Passat<sup>3</sup>

<sup>1</sup> Université de Strasbourg, CNRS, ICube, France

<sup>2</sup> Université Paris-Descartes, LIPADE, France

<sup>3</sup> Université de Reims Champagne-Ardenne, CReSTIC, France

**Abstract**—The binary partition tree (BPT) is a well-known hierarchical data-structure, frequently involved image segmentation procedures. The efficiency of segmentation based on BPTs depends on the segmentation process (“how to use a BPT?”), but also on the quality of the data-structure (“how to build a BPT?”). In this article, we propose a scheme for BPT quality analysis, with the purpose of answering the latter question. It relies on the observation of the very structure of a BPT, with respect to a given ground-truth example. Our hypothesis is that such intrinsic scheme can bring relevant clues about the ability of a BPT to provide correct segmentation results. Experiments carried out on satellite images illustrate the relevance of this scheme.

**Index Terms**—Binary partition tree, supervised quality evaluation, image segmentation, mathematical morphology.

## I. INTRODUCTION

The Binary Partition Tree (BPT) [1] is a hierarchical data-structure that can be used for image modelling. It is a binary tree that can represent the image content at different levels of detail. By contrast to other hierarchical models (see, e.g., [2]–[7]) mostly built from the only information contained in the image, the BPT construction relies both on the information embedded in the image, and on external information, namely a prior knowledge related to the structures of interest.

When BPTs are involved in segmentation procedures, the quality of the result then depends on the way to *handle* the BPT (for defining an optimal partition of the image support), but also the way to *build* this BPT. This construction step is crucial. Indeed, a badly constructed BPT will not allow for a good segmentation result, by providing an non-adapted search space. In other words, when considering BPT-based image segmentation, a good segmentation algorithm has to be applied on a good image tree data-structure.

Many articles have been devoted to BPT-based segmentation, especially for remote sensing [8]–[16]. In this context, various metrics were investigated (spectral, spatial, geometric, etc.) for embedding a prior knowledge. Their design strongly influences the resulting hierarchical structures and thus the quality of the subsequent segmentation results. But, surprisingly, there exist very few works devoted to evaluate the capacity of a BPT to provide relevant segmentation results.

It is fundamental to distinguish *segmentation evaluation*, which has been widely investigated (e.g., in [17]–[22]), and *BPT evaluation*. Indeed, the latter is the evaluation of a search space of putative segmentation results; the purpose is then to

help the user to choose a right BPT, not to use it the right way. To the best of our knowledge, the only framework for assessing the quality of a hierarchy of partitions for segmentation purpose was proposed in [23]. It consists of selecting, in the tree, a set of segments matching an ideal partition that is forced to be in the hierarchy; its selection is expressed as a linear fractional combinatorial optimisation problem. Such approach requires a full ground-truth partition of the image whereas only partial segments representing some objects of interest may be available for some particular applications.

Our purpose is to evaluate the quality of a BPT or, equivalently, its construction process. In this paper, we aim to show that reliable clues for such a quality analysis can be obtained by directly investigating the BPT structure with respect to partial ground-truth (GT) examples. Indeed, our hypothesis is that a BPT provides —by its inner structure and its spatial embedding in the image support— some information about its relevance and its ability to extract specific objects of interest.

This article is organised as follows. In Section II, we first remind some background notions related to the BPT. Then, in Section III, we present an example-based subtree extraction for reducing the data-space to consider for each GT example. In Section IV, a pre-processing is presented, in order to estimate the relevance of the intrinsic quality analysis. Combinatorial and quantitative analyses are then proposed, in Section V, for intrinsic BPT quality evaluation. In Section VI, experiments on remote sensing images are described.

## II. BINARY PARTITION TREE

An image  $I$  is defined on a set of points  $\Omega$ . These points are spatially organized; this is modelled by a neighbourhood relationship, i.e. an adjacency (irreflexive, symmetric) relation  $\curvearrowright$  on  $\Omega$ . A BPT associated to the graph  $(\Omega, \curvearrowright)$  is a tree  $\mathfrak{T} = (\mathcal{N}, \searrow)$ , i.e. a directed, connected, acyclic graph ( $\searrow$  reflects the construction link between nodes). The set  $\mathcal{N}$  is partitioned into three subsets:  $\mathcal{R} = \{N_\Omega\}$  such that  $N_\Omega = \Omega$ ;  $\mathcal{B} \subset 2^\Omega$ ; and  $\mathcal{L} = \{N_x\}_{x \in \Omega}$  such that  $\forall x \in \Omega, N_x = \{x\}$ . The nodes of these subsets satisfy the following properties:

$$\forall N \in \mathcal{R} \cup \mathcal{B}, d^+(N) = 2 \quad (1)$$

$$\forall N \in \mathcal{L}, d^+(N) = 0 \quad (2)$$

$$\forall N \in \mathcal{B} \cup \mathcal{L}, d^-(N) = 1 \quad (3)$$

$$\forall N \in \mathcal{R}, d^-(N) = 0 \quad (4)$$

$$\forall N \in \mathcal{R} \cup \mathcal{B}, N = \bigcup_{N' \searrow N} N' \quad (5)$$

This work was partially supported by the French *Agence Nationale de la Recherche* under grants ANR-12-MONU-0001, ANR-15-CE23-0009 and ANR-17-CE23-0015.

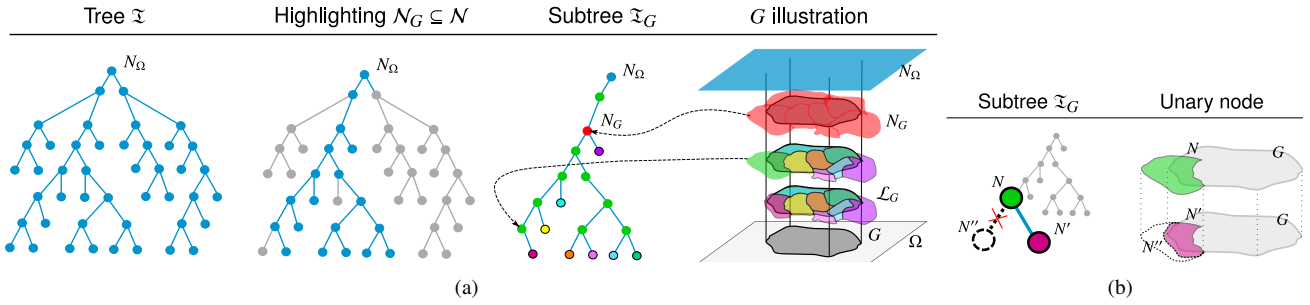


Fig. 1. (a) Illustration of subtree extraction where  $\mathfrak{T}$  is the whole tree,  $N_\Omega$  is its root,  $\mathcal{L}_G$  is the set of leaves intersecting the GT example  $G$ .  $\mathfrak{T}_G$  is the subtree of interest, and  $N_G$  is its actual root. (b) Example of a unary node  $N$  where  $N \searrow N'$  and  $N \cap G = N' \cap G$ , while  $N' \subset N$ . The only other node  $N'' \subset N$  such that  $N \searrow N''$  does not intersect  $G$ .

where  $d^+(N) = |\{N' \in \mathcal{N}, N \searrow N'\}|$  and  $d^-(N) = |\{N' \in \mathcal{N}, N' \searrow N\}|$ . A BPT  $\mathfrak{T}$  of  $(\Omega, \prec)$  provides a family  $\mathcal{N}$  of subsets of  $\Omega$ . These subsets are hierarchically organised from the whole set  $\Omega$ , to the singleton sets  $\{x\}$ ,  $x \in \Omega$ , with respect to the inclusion relation. This hierarchical organisation is characterised by the fact that an element  $N$  of  $\mathcal{N}$  is associated, via  $\searrow$ , to exactly two elements  $N_1, N_2$  of  $\mathcal{N}$  that form a binary partition of  $N$ . In other words, we have  $N = N_1 \cup N_2$ ,  $N_1 \cap N_2 = \emptyset$  and  $N_1, N_2 \neq \emptyset$ . The elements of  $\mathcal{N}$  are the *nodes* of  $\mathfrak{T}$ , the node  $\Omega$  is the *root* of  $\mathfrak{T}$ , the singleton nodes of  $\mathcal{L}$  are the *leaves* of  $\mathfrak{T}$ .

### III. EXAMPLE-BASED SUBTREE EXTRACTION

Our purpose is to evaluate how well a BPT  $\mathfrak{T}$  is adapted to provide nodes matching with a segment representing a GT example  $G$ . Some nodes of  $\mathcal{N}$  do not intersect  $G$ ; in such case, they are useless for the analysis with respect to  $G$ . Then, we focus only on the nodes  $N \in \mathcal{N}$  such that  $N \cap G \neq \emptyset$ . Their subset is computed, in a bottom-up fashion, by first selecting all the leaves  $L \in \mathcal{L}$  that intersect  $G$ , and then preserving iteratively all the parent nodes connected to any such leaves by the  $\searrow$  relation, until the root  $N_\Omega$  (Fig. 1(a)).

The obtained subset of nodes  $\mathcal{N}_G \subseteq \mathcal{N}$  induces a subtree  $\mathfrak{T}_G$  of  $\mathfrak{T}$ , of root  $N_\Omega$  and of leaves  $\mathcal{L}_G = \{L \in \mathcal{L} \mid L \cap G \neq \emptyset\}$ . This subtree *may not be binary*. Indeed, there may exist nodes  $N \in \mathcal{N}_G$  that have one child  $N' \in \mathcal{N}_G$  (i.e.,  $N \searrow N'$ ). (This happens when the only other node  $N'' \subset N$  such that  $N \searrow N''$  does not intersect  $G$ .) Such nodes  $N$  are called *unary nodes* (Fig. 1(b)), by contrast with the other *binary nodes* that do have two children nodes in  $\mathcal{N}_G$ .

The intersection of a unary node  $N$  with  $G$  is the same as for its only child  $N'$ : if  $N \searrow N'$ , we have  $N \cap G = N' \cap G$ , while  $N' \subset N$ . Then, a unary node increases the amount of false positive (FP) material with respect to  $G$ , compared to its descendants. In particular, this is true in the upper part of the tree  $\mathfrak{T}_G$ , between the root  $N_\Omega$  and the first binary node  $N_G$  of  $\mathfrak{T}_G$ . Indeed, there exists, within  $\mathcal{N}_G$ , a sequence of successive nodes  $N_\Omega = N_0 \searrow N_1 \searrow \dots \searrow N_k = N_G$  ( $k \geq 0$ ) such that all  $N_i$  ( $0 \leq i < k$ ) are unary. We can relevantly remove from  $\mathfrak{T}_G$  all these nodes  $N_i$  and only preserve, as pseudo-root, the first binary node  $N_G$  (red node in Fig. 1(a)). By construction,  $N_G$  is the smallest node of  $\mathcal{N}$  that includes  $G$ .

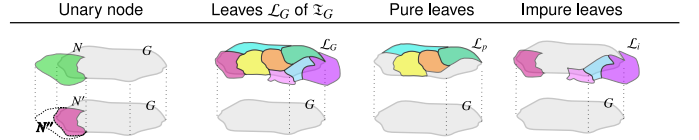


Fig. 2. A unary node (impure) and sets of pure and impure leaves.

The final subtree (still noted  $\mathfrak{T}_G$ ) contains all the nodes of interest of  $\mathfrak{T}$ , with respect to the GT example  $G$ . Its combinatorial analysis then allows us to obtain information about the quality of the BPT  $\mathfrak{T}$ .

### IV. RELEVANCE OF THE INTRINSIC QUALITY ANALYSIS

A BPT  $\mathfrak{T}$  is built in a bottom-up fashion. The construction process starts from the set of leaves  $\mathcal{L}$  and progressively creates new nodes by iteratively merging pairs of adjacent nodes. These pairs are chosen with respect to a given metric, and the inclusion relation between two nodes and their merged union practically defines the  $\searrow$  relation.

The initial set of leaves is often chosen as  $\mathcal{L} = \{N_x\}_{x \in \Omega}$ , i.e. each leaf corresponds to exactly one point of the image. For practical reasons,  $\mathcal{L}$  can sometimes be defined as a set of larger nodes (e.g., flat zones or superpixels). This partition is generally non-correlated to the node-merging strategy. Nevertheless, it has an important impact on the relevance of the proposed evaluation framework. In particular, two properties of this initial partition are crucial.

a) *Granularity*: The granularity  $\gamma$  is defined as the ratio between the size of  $G$  (number of points) and the size of  $\mathcal{L}_G$  (number of leaves). It is defined as

$$\gamma = \frac{|\mathcal{L}_G|}{|G|} \quad (6)$$

and lies in  $]0, 1]$ . *The higher the granularity, the most relevant the intrinsic quality analysis carried out on  $\mathfrak{T}_G$ .* Indeed, for  $\gamma = 1$ , the number of leaves that intersect  $G$  is equal to the number of points of  $G$ . Then, each leaf contains exactly one point of  $G$ , and the ability of the BPT to allow for a segmentation that correctly fits  $G$  highly depends on the way to merge the nodes. By contrast, if  $\gamma = 1/|G|$ , then one leaf

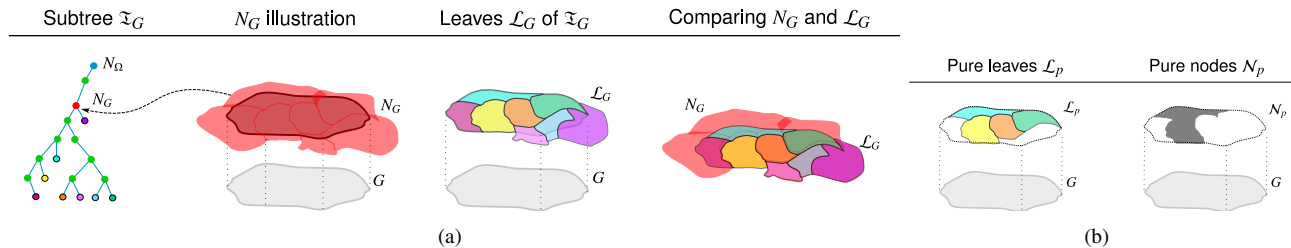


Fig. 3. (a) Comparison between the amount of points in the root  $N_G$  of  $\mathfrak{T}_G$  and the amount of points that could be theoretically obtained from the initial partition of the leaves  $\mathcal{L}_G$ . (b) The set  $\mathcal{L}_p$  of pure leaves and the set  $\mathcal{N}_p$  of pure nodes, maximal with respect to the  $\subseteq$  relation. The white regions represent  $|G| - (\sum_{L \in \mathcal{L}_p} |L|)$  (on the left), and  $|G| - (\sum_{N \in \mathcal{N}_p} |N|)$  (on the right).

already includes  $G$ , and the way of further building  $\mathfrak{T}_G$  has no influence on the segmentation of  $G$ .

b) *Discordance*: The discordance  $\delta$  is defined as the relative quantitative error on the size of  $G$  induced by  $\mathcal{L}_G$ . It is defined as

$$\delta = \frac{1}{|G|} \sum_{L \in \mathcal{L}_G, L \not\subseteq G} \min\{|L \setminus G|, |L \cap G|\} \quad (7)$$

and lies in  $[0, 1]$ . *The lowest the discordance, the most relevant the intrinsic quality analysis carried out on  $\mathfrak{T}_G$ .* Indeed,  $\delta = 0$  means that the initial partition provides a set of leaves that perfectly fits  $G$ . Then, the quality of the BPT directly depends on the ability to merge these nodes. By contrast,  $\delta \approx 1$  means that many leaves of  $\mathcal{L}$  partially intersect both  $G$  and the remainder of  $\Omega$ . Then, the ability to finally obtain a “good” segmentation of  $G$  is low and weakly depends on the ability to merge the nodes when building  $\mathfrak{T}$ .

For  $G$  sufficiently large, a high value of granularity implies a low value of discordance. However, the counterpart is not true: a low value of discordance can be obtained for a low value of granularity. Note that when the initial partition is composed of leaves that are points of the image, we have  $\gamma = 1$  and  $\delta = 0$ . In such case, the quality of the BPT only depends on the node merging process.

## V. INTRINSIC QUALITY ANALYSIS

### A. Combinatorial analysis

The subtree  $\mathfrak{T}_G$  is composed of  $n$  nodes (including 1 root and  $l$  leaves) and  $n - 1$  edges  $\searrow$ . Observing the status of these nodes provides us with quality clues of the BPT.

A node  $N \in \mathcal{N}_G$  is *pure* (resp. *impure*) if  $N \subseteq G$  (resp.  $N \not\subseteq G$ ). The classification of the leaves of  $\mathcal{L}_G$  into pure / impure can be done by observing their support, compared to  $G$  (Fig. 2). We set  $l_p$  (resp.  $l_i$ ) the number of pure (resp. impure) leaves, respectively (we have  $l_p + l_i = l$ ). The purity / impurity of the other nodes can then be computed iteratively: if  $N \in \mathcal{N}_G$  is a unary node, then it is impure; if  $N \in \mathcal{N}_G$  is a binary node, with  $N \searrow N', N''$ , it is pure if  $N'$  and  $N''$  are pure, otherwise it is impure.

A “good” BPT construction should preserve as much as possible the purity of nodes; avoid to merge pure and impure nodes; and avoid to increase the size of impure nodes. Thus:

- the merging in  $\mathfrak{T}$  leading to a unary node in  $\mathfrak{T}_G$  is a bad operation, as it creates from impure —and sometimes pure— nodes, an impure node with a greater amount of points out of  $G$ ;
- the merging in  $\mathfrak{T}$  leading to a binary node from two pure nodes in  $\mathfrak{T}_G$  is a good operation, as it allows one to converge towards  $G$ ;
- the merging in  $\mathfrak{T}$  leading to a binary node from two impure nodes in  $\mathfrak{T}_G$  is a good operation, as it neither deteriorates pure areas, nor increases the amount of points out of  $G$ ;
- the merging in  $\mathfrak{T}$  leading to a binary node from a pure and an impure node in  $\mathfrak{T}_G$  is a bad operation, as it makes the result diverging from  $G$ .

It is possible to count the number of each kind of nodes:  $u_i$ ,  $b_{pp}$ ,  $b_{ii}$  and  $b_{pi}$ , for the unary nodes, and binary nodes built from pure-pure, impure-impure, pure-impure couples. We have  $u_i + b_{pp} + b_{ii} + b_{pi} + l_p + l_i = n$ , and a good BPT should minimise  $u_i$  and  $b_{pi}$ , while maximising  $b_{pp}$  and  $b_{ii}$ . In particular, a “perfect” BPT should satisfy:

$$u_i = 0 \quad (8)$$

$$b_{pp} = l_p - 1 \quad (9)$$

$$b_{ii} = l_i - 1 \quad (10)$$

$$b_{pi} = 1 \quad (11)$$

(except when  $l_i = 0$ , where  $b_{pp}$  should be equal to  $l - 1$ , and all others to 0).

From this classification of nodes, and the combinatorial analysis of their population, it is then possible to build a wide range of structural measures that quantify the difference of quality between BPTs. Examples of such measures will be proposed in Section VI.

### B. Quantitative analysis

A quantitative assessment of the quality of the BPT can also be carried out by observing the lowest set including  $G$  and the greatest set included in  $G$  which can be built from  $\mathfrak{T}_G$ .

Let us first focus on the lowest set including  $G$ . By construction, it is the root of  $\mathfrak{T}_G$ , namely  $N_G$ . The interesting information carried by  $N_G$  is the amount of points outside of  $G$  (Fig. 3(a)). More precisely, this amount  $|N_G| - |G|$  has to be compared to the amount that could be theoretically

obtained from the initial partition of the leaves  $\mathcal{L}_G$ , namely  $(\sum_{L \in \mathcal{L}_G} |L|) - |G|$ . Computing the difference, or the ratio, between these two values allows us to assess the quantitative error related to the existence of unary nodes in  $\mathfrak{T}_G$ , i.e. the addition of non-relevant zones to the expected exhaustive segmentation of  $G$ . The lower this value, the better the ability of the BPT to take advantage of the adequacy of the initial partition to the GT segment. Second, let us focus on the greatest set included in  $G$  (Fig. 3(b)). It is defined as the union of all the pure nodes of  $\mathcal{N}_G$  whose parents are impure; we note this set  $\mathcal{N}_p$ . The first interesting value is the amount of points of  $G$  outside this pure set:  $|G| - (\sum_{N \in \mathcal{N}_p} |N|)$ . It can be compared to the amount of  $G$  outside the best theoretical pure subset that could be obtained from the leaves, i.e.  $|G| - (\sum_{L \in \mathcal{L}_p} |L|)$ , where  $\mathcal{L}_p = \{L \in \mathcal{L} \mid L \subseteq G\}$ . The lower this value, the better the ability of the BPT to take advantage of the potential adequacy of the initial partition to the GT segment. The second interesting value of interest is the size of  $\mathcal{N}_p$ , i.e. number of nodes required to form the best segmentation lower than  $G$ . The lower this value, the better the ability of the BPT to avoid over-segmentation.

Of course, these two values have to be considered jointly. Indeed, a low value of  $|\mathcal{N}_p|$  is not meaningful if the union of the nodes of  $\mathcal{N}_p$  is highly degraded with respect to the initial partition. Similarly, an optimal union of the nodes of  $\mathcal{N}_p$  is meaningless if these nodes are numerous (i.e., could not be merged together by the BPT, and were instead fused into impure greater nodes).

## VI. EXPERIMENTAL STUDY

In this section, our aim is to emphasise in which extent our intrinsic analysis framework can be used for the quality evaluation of BPTs. In particular, it may be seen as a companion tool for the extrinsic analysis framework proposed in [24].

### A. Experimental protocol

Our experiments use a crop (500<sup>2</sup> pixels) of Fig. 4(a). We consider 3 types of BPTs:  $BPT_{std}$ ,  $BPT_{ndvi}$  and  $BPT_{ndwi}$ , each one built using a metric based on the radiometric intensity, the Normalized Difference Vegetation (NDVI) and Water Indices (NDWI), respectively. In order to show the influence of the initial partition  $\mathcal{L}$  on the intrinsic evaluation analysis, 4 BPTs are built for each type, by using various initial partitions:  $\mathcal{L}_1$  is composed of all pixels from the image support (250 000 regions);  $\mathcal{L}_2$  is composed of 18 750 regions;  $\mathcal{L}_3$  is composed of 12 500 regions; and  $\mathcal{L}_4$  is composed of 6 250 regions.

When  $\gamma$  and  $\delta$  are satisfactory, we use our framework to estimate the ability of these BPTs to generate potential nodes well matching a set  $\mathcal{L}_G$  of 13 GT examples from each we extract a subtree  $\mathfrak{T}_G$ . Examples of GT examples are illustrated in Fig. 5.

To obtain values normalised in  $[0, 1]$ , we define two scores

$$cb_1 = (b_{pp} + b_{ii}) / (u_i + b_{pp} + b_{ii} + b_{pi}) \quad (12)$$

$$cb_2 = b_{pp} / (b_{pp} + b_{pi}) \quad (13)$$

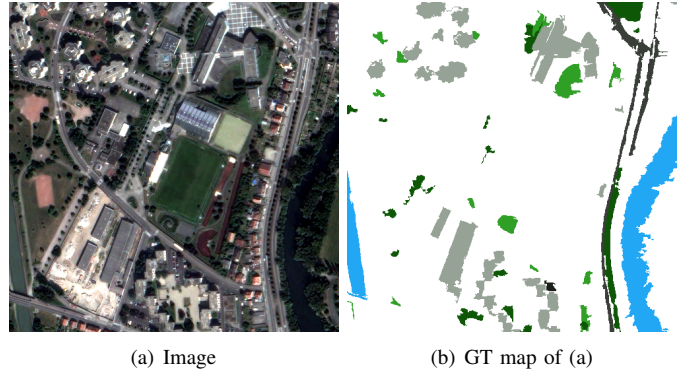


Fig. 4. (a) Satellite image at a spatial resolution of 60 cm. (b) GT map with reference segments belonging to 5 (coloured) semantic classes.

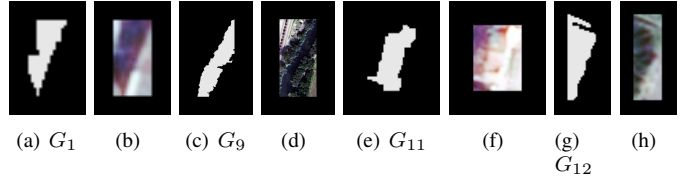


Fig. 5. Examples of 4 GT segments, with their binary masks (a, c, e, g) and the image around them ((b)  $G_1$ , (d)  $G_9$ , (f)  $G_{11}$ , (h)  $G_{12}$ ).

The closer these values from 1 (resp. 0), the more (resp. less) acceptable the BPTs. In particular, for a GT example, we assume that a BPT provides an acceptable matching region if these scores are higher than 0.5.

We used the definitions proposed in Section V-B for the quantitative analysis. For a better readability, we set

$$qt_1 = |N_G \setminus G| - |(\bigcup_{L \in \mathcal{L}_G} L) \setminus G| = |N_G \setminus \bigcup_{L \in \mathcal{L}_G} L| \quad (14)$$

$$qt_2 = |N_G \setminus G| / |(\bigcup_{L \in \mathcal{L}_G} L) \setminus G| \quad (15)$$

We also simplify some notations by using  $\nu_p = (\sum_{N \in \mathcal{N}_p} |N|)$  and  $\lambda_p = (\sum_{L \in \mathcal{L}_p} |L|)$ . Thus, we can define

$$qt_3 = (|G| - \nu_p) - (|G| - \lambda_p) = \lambda_p - \nu_p \quad (16)$$

$$qt_4 = |\mathcal{N}_p| \quad (17)$$

### B. Results and discussion

Table I presents the combinatorial scores obtained from  $BPT_{std}$ , built from the initial partition  $\mathcal{L}_1$ . By construction of  $\mathcal{L}_1$ , the values of  $\gamma$  and  $\delta$  are optimal. We can notice that the scores are generally around 0.9 and above 0.5, namely our point of reference. This suggests that the intrinsic structure of  $BPT_{std}$  can provide acceptable segmentation results for the GT examples  $G_1$ ,  $G_9$ ,  $G_{11}$  and  $G_{12}$ . We can observe that the  $cb_1$  and the  $cb_2$  scores are high. Indeed, the values of  $u_i$ ,  $b_{pp}$ ,  $b_{ii}$  and  $b_{pi}$  are not far from the values that correspond to a perfect BPT (see Eqs. (8–11)).

Table II presents some statistical information about various  $BPT_{std}$  built using  $\mathcal{L}_1$ ,  $\mathcal{L}_2$ ,  $\mathcal{L}_3$  and  $\mathcal{L}_4$  as initial partitions,

with respect to the GT segment  $G_1$ . The values of  $cb_1$  and  $cb_2$  for the first and the third lines suggest that the BPTs built by using  $\mathcal{L}_1$  is able to provide acceptable matching regions for the GT example  $G_1$  while the other BPTs are not. The low scores of the BPTs built by using  $\mathcal{L}_2$ ,  $\mathcal{L}_3$  and  $\mathcal{L}_4$  are correlated with the non-optimal values of  $\gamma$  that are far from 1.

From another point of view, the values in Table III show the differences between the various BPTs: one of them induces a lower amount of unary nodes ( $BPT_{std}$ ) compared to the others ( $BPT_{ndvi}$ ,  $BPT_{ndwi}$ ). This suggests that the hierarchical structure of the  $BPT_{std}$ , for the GT example  $G_1$ , is likely to better provide acceptable segment matching.

For a first quantitative analysis, Table IV gives information about the absolute ( $qt_1$ ) and relative ( $qt_2$ ) amount of false positives, induced by the construction of the BPT. The lower these values, the better the ability of the BPT to use at best the potential adequacy of the initial partition to the GT segment. Here, the  $BPT_{std}$  built from the initial partition  $\mathcal{L}_2$  only provides interesting prediction for the GT example  $G_1$ , where the estimated false positives ( $qt_1 = 62$ ) are less than the half of the size of the GT example. In the other cases, we observe a high difference between the size of the chosen root of the subtree and the size of the GT segment. In the context of urban imaging, the excessive size of these roots can be explained by the presence of disturbing objects (e.g., shadows, spots on the roof) that make small pieces of regions more similar to other far located objects than to their neighbours. Those kinds of segments tend to not fuse rapidly with their neighbours and often persist until the end of the BPT construction.

In Table V, we observe that, for  $BPT_{std}$ , the size  $|N_G|$  of the selected root is close to that of  $|G|$  for the GT segment  $G_1$ . The values of  $qt_1$  for this GT then suggest that the numbers of points representing potential false positives when segmenting are not high compared to the values for  $BPT_{ndvi}$  and  $BPT_{ndwi}$ . This result shows that the use of the metric based on radiometric intensities is more relevant for this study. This is probably due to the fact that the studied image contains urban objects, with a corresponding GT map mainly composed of built areas. Then, the metrics based on NDVI and NDWI are weakly adapted for the detection of such kinds of objects.

A second quantitative analysis aims to estimate the amount of false negative points induced by the construction process. Table VI presents quantitative information about the subtrees extracted from the  $BPT_{std}$  built from an initial partition  $\mathcal{L}_3$ . The score  $qt_3$  estimates the increase of false negative points during the construction process of the tree, while  $qt_4$  shows the relevance of each subtree by showing the number of maximal pure nodes well merged in the hierarchical structure.

For the GT example  $G_{12}$  (Fig. 5(d)), the values of  $|G| - \nu_p$  are visually illustrated in Fig. 6, showing in orange the set of subregions that are already well-formed in the extracted subtree. We notice both from Table VII and Fig. 6 that the hierarchical structure of the subtrees extracted from the three types of BPTs are interesting since they generate matching subregions with fair size. The values of  $qt_4$  in Table VII suggest that the  $BPT_{ndvi}$  and the  $BPT_{ndwi}$  may not be

TABLE I  
COMBINATORIAL QUALITY SCORES OF  $BPT_{std}$  BUILT FROM  $\mathcal{L}_1$  ( $\gamma = 1$ ,  $\delta = 0$ ,  $l_i = 0$ ). THE 4 LINES CORRESPOND TO  $G_1$ ,  $G_9$ ,  $G_{11}$  AND  $G_{12}$ . THE BEST THEORETICAL VALUES ARE BETWEEN BRACKETS.

$l_p$	$u_i$	$b_{pp}$	$b_{ii}$	$b_{pi}$	$cb_1$	$cb_2$
182	17 (0)	166 (181)	5 (0)	10 (0)	0.86	0.94
22378	378 (0)	22019 (22377)	129 (0)	229 (0)	0.97	0.99
566	105 (0)	534 (565)	14 (0)	17 (0)	0.82	0.97
541	48 (0)	512 (540)	11 (0)	17 (0)	0.89	0.97

TABLE II  
COMBINATORIAL QUALITY SCORES FOR  $BPT_{std}$  BUILT FROM  $\mathcal{L}_1$  TO  $\mathcal{L}_4$  (FROM THE 1ST TO THE 4TH LINE), WITH RESPECT TO  $G_1$ .

$\gamma$	$\delta$	$l_i$	$l_p$	$u_i$	$b_{pp}$	$b_{ii}$	$b_{pi}$	$cb_1$	$cb_2$
1.00	0.00	0	182	17 (0)	166 (181)	5 (0)	10 (0)	0.86	0.94
0.06	0.06	5	6	8 (0)	2 (5)	5 (4)	3 (1)	0.39	0.40
0.04	0.06	5	3	7 (0)	1	5 (4)	1 (1)	0.43	0.50
0.02	0.09	3	1	5 (0)	0 (0)	3 (2)	0 (1)	0.38	0.00

TABLE III  
COMBINATORIAL QUALITY SCORES OF THREE BPTs BUILT FROM  $\mathcal{L}_1$ , WITH RESPECT TO  $G_1$  ( $\gamma = 1$ ,  $\delta = 0$ ,  $l_i = 0$  AND  $l_p = 182$ ).

BPT	$u_i$	$b_{pp}$	$b_{ii}$	$b_{pi}$	$cb_1$	$cb_2$
$BPT_{std}$	17 (0)	166 (181)	5 (0)	10 (0)	0.864	0.943
$BPT_{ndvi}$	83 (0)	131 (181)	16 (0)	34 (0)	0.557	0.794
$BPT_{ndwi}$	82 (0)	133 (181)	12 (0)	36 (0)	0.551	0.787

TABLE IV  
QUANTITATIVE QUALITY ANALYSIS OF  $BPT_{std}$  BUILT FROM  $\mathcal{L}_2$ .  $L_G$  REFERS TO  $L \in \mathcal{L}_G$ . THE 4 LINES CORRESPOND TO  $G_1$ ,  $G_9$ ,  $G_{11}$  AND  $G_{12}$ , RESPECTIVELY.

$ G $	$ N_G $	$ N_G \setminus G $	$ \bigcup L_G \setminus G $	$qt_1$	$qt_2$
182	259	77	15	62	5.133
22378	75948	53570	605	52965	88.545
566	101525	100959	78	100881	1294.346
541	30894	30353	67	30286	453.030

TABLE V  
QUANTITATIVE QUALITY SCORES OF BPTs BUILT FROM  $\mathcal{L}_1$ , W.R.T.  $G_1$ . WE HAVE  $|\bigcup_{L \in \mathcal{L}_G} L \setminus G| = 0$ ; SO WE CANNOT COMPUTE  $qt_2$ .

BPT	$ G $	$ N_G $	$ N_G \setminus G $	$qt_1$
$BPT_{std}$	182	259	77	77
$BPT_{ndvi}$	182	30302	30120	30120
$BPT_{ndwi}$	182	20490	20308	20308

TABLE VI  
QUANTITATIVE QUALITY ANALYSIS OF  $BPT_{std}$  OBTAINED FROM  $\mathcal{L}_3$ . THE 4 LINES CORRESPOND TO  $G_1$ ,  $G_9$ ,  $G_{11}$  AND  $G_{12}$ , RESPECTIVELY.

$ G $	$\nu_p$	$\lambda_p$	$ G  - \nu_p$	$ G  - \lambda_p$	$qt_3$	$qt_4$
182	25	43	157	139	18	1
22378	20803	21603	1575	775	800	69
566	505	539	61	27	34	11
541	423	453	118	88	30	3

TABLE VII  
QUANTITATIVE QUALITY SCORES OF BPTs BUILT FROM  $\mathcal{L}_1$ , W.R.T.  $G_{12}$ .

BPT	$ G $	$\nu_p$	$\lambda_p$	$ G  - \nu_p$	$ G  - \lambda_p$	$qt_3$	$qt_4$
$BPT_{std}$	541	531	541	10	0	10	19
$BPT_{ndvi}$	541	496	541	45	0	68	73
$BPT_{ndwi}$	541	509	541	32	0	32	30

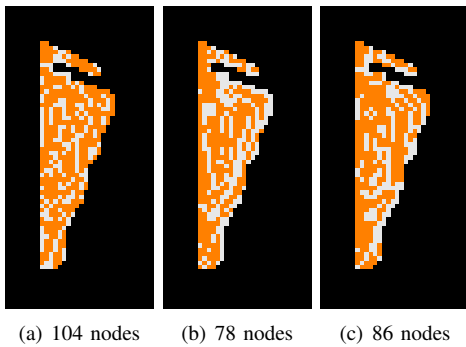


Fig. 6. Maximal pure nodes of the subtrees, in orange, with respect to the GT example  $G_{12}$ , extracted from the BPTs obtained by using the initial partitions  $\mathcal{L}_1$ : (a) for  $BPT_{std}$ ; (b) for  $BPT_{ndvi}$ ; (c) for  $BPT_{ndwi}$ .

relevant for the GT segment  $G_{12}$ . Indeed, the values of  $qt_4$  are high, while the amount  $qt_3$  of false negative points is acceptable although the set of maximal pure nodes almost matches with the GT example  $G_{12}$  (see Fig. 6). For a case where the value of  $qt_3$  may be the best for a BPT, its high value of  $qt_4$  predicts a high risk of potential bad node fusions.

## VII. CONCLUSION

In this paper, we proposed a scheme for BPT quality analysis, by observing the intrinsic information contained in the hierarchical data-structure. With respect to a set of user-defined GT segments, it may help to better understand the potential results that we can obtain from the BPTs. Experiments, on examples of combinatorial and quantitative analysis on remote sensing images, illustrate how the intrinsic information of a BPT can lead to the estimation of its potential usefulness for further segmentation process. It is important to notice that the relevance of this analysis highly depends on the initial partition used during the construction of the BPT (see Section IV). When such partitions are correctly chosen, the proposed framework then provides us with relevant intrinsic information about the quality of BPTs, and can then be used as a fair prospective or retrospective evaluation tool.

As a perspective of this work, extending the proposed strategy to multiple GT examples will be interesting since the evaluation will be done for a partial partition containing (non-)connected segments of reference. In [24], we proposed a scheme for extrinsic analysis of the quality of the BPTs allowing the user to use various metrics of quality. Coupling these two—intrinsic and extrinsic—schemes will be relevant since it will give access to a more complete evaluation of the quality of the BPTs in the context of image segmentation. Adapting the proposed method to other kinds of hierarchies will also be investigated, opening the gate to other applications.

## REFERENCES

[1] P. Salembier and L. Garrido, “Binary partition tree as an efficient representation for image processing, segmentation, and information retrieval,” *IEEE Trans. Image Proc.*, vol. 9, pp. 561–576, 2000.  
 [2] L. Najman and M. Schmitt, “Geodesic saliency of watershed contours and hierarchical segmentation,” *IEEE Trans. Patt. Anal. Mach. Intell.*, vol. 18, pp. 1163–1173, 1996.

[3] P. Salembier, A. Oliveras, and L. Garrido, “Anti-extensive connected operators for image and sequence processing,” *IEEE Trans. Image Proc.*, vol. 7, pp. 555–570, 1998.  
 [4] P. Monasse and F. Guichard, “Scale-space from a level lines tree,” *J. Vis. Comm. Image Rep.*, vol. 11, pp. 224–236, 2000.  
 [5] B. Perret, S. Lefèvre, C. Collet, and E. Slezak, “Hyperconnections and hierarchical representations for grayscale and multiband image processing,” *IEEE Trans. Image Proc.*, vol. 21, pp. 14–27, 2012.  
 [6] C. Kurtz, B. Naegel, and N. Passat, “Connected filtering based on multivalued component-trees,” *IEEE Trans. Image Proc.*, vol. 23, pp. 5152–5164, 2014.  
 [7] E. Carlinet and T. Géraud, “MToS: A tree of shapes for multivariate images,” *IEEE Trans. Image Proc.*, vol. 24, pp. 5330–5342, 2015.  
 [8] J. A. Benediktsson, L. Bruzzone, J. Chanussot, M. Dalla Mura, P. Salembier, and S. Valero, “Hierarchical analysis of remote sensing data: Morphological attribute profiles and binary partition trees,” in *ISMM, Procs.*, 2011, pp. 306–319.  
 [9] A. Alonso-González, C. López-Martínez, and P. Salembier, “Filtering and segmentation of polarimetric SAR data based on binary partition trees,” *IEEE Trans. Geosc. Rem. Sens.*, vol. 50, pp. 593–605, 2012.  
 [10] C. Kurtz, N. Passat, P. Gañçarski, and A. Puissant, “Extraction of complex patterns from multiresolution remote sensing images: A hierarchical top-down methodology,” *Patt. Rec.*, vol. 45, pp. 685–706, 2012.  
 [11] M. A. Veganzones, G. Tochon, M. Dalla Mura, A. J. Plaza, and J. Chanussot, “Hyperspectral image segmentation using a new spectral unmixing-based binary partition tree representation,” *IEEE Trans. Image Proc.*, vol. 23, pp. 3574–3589, 2014.  
 [12] A. Alonso-González, C. López-Martínez, and P. Salembier, “PolSAR time series processing with binary partition trees,” *IEEE Trans. Geosc. Rem. Sens.*, vol. 52, pp. 3553–3567, 2014.  
 [13] P. Salembier, “Study of binary partition tree pruning techniques for polarimetric SAR images,” in *ISMM, Procs.*, 2015, pp. 51–62.  
 [14] S. Valero, P. Salembier, and J. Chanussot, “Object recognition in hyperspectral images using binary partition tree representation,” *Patt. Rec. Lett.*, vol. 56, pp. 45–51, 2015.  
 [15] E. Maggiori, Y. Tarabalka, and G. Charpiat, “Optimizing partition trees for multi-object segmentation with shape prior,” in *BMVC, Procs.*, 2015.  
 [16] —, “Improved partition trees for multi-class segmentation of remote sensing images,” in *IGARSS, Procs.*, 2015, pp. 1016–1019.  
 [17] H. Vojodi and A. M. E. Moghadam, “A supervised evaluation method based on region shape descriptor for image segmentation algorithm,” in *AISP, Procs.*, 2012, pp. 18–22.  
 [18] J. Pont-Tuset and F. Marques, “Measures and meta-measures for the supervised evaluation of image segmentation,” in *CVPR, Procs.*, 2013, pp. 2131–2138.  
 [19] H. Li, J. Cai, T. Nguyen, and J. Zheng, “A benchmark for semantic image segmentation,” in *ICME, Procs.*, 2013, pp. 1–6.  
 [20] A. Troya-Galvis, P. Gañçarski, N. Passat, and L. Berti-Équille, “Unsupervised quantification of under- and over-segmentation for object-based remote sensing image analysis,” *IEEE J. Sel. Top. App. Earth Obs. Rem. Sens.*, vol. 8, pp. 1936–1945, 2015.  
 [21] J. Pont-Tuset, P. Arbelaez, J. Barron, F. Marques, and J. Malik, “Multiscale combinatorial grouping for image segmentation and object proposal generation,” *IEEE Trans. Patt. Anal. Mach. Intell.*, vol. 39, pp. 128–140, 2017.  
 [22] J. Pont-Tuset and F. Marques, “Supervised evaluation of image segmentation and object proposal techniques,” *IEEE Trans. Patt. Anal. Mach. Intell.*, vol. 38, pp. 1465–1478, 2016.  
 [23] —, “Supervised assessment of segmentation hierarchies,” in *ECCV, Procs.*, 2012, pp. 814–827.  
 [24] J. F. Randrianasoa, C. Kurtz, É. Desjardin, P. Gañçarski, and N. Passat, “Supervised evaluation of the quality of binary partition trees based on uncertain semantic ground-truth for image segmentation purpose,” in *ICIP, Procs.*, 2017, pp. 3874–3878.